An overview of wavelet transform concepts and applications

Christopher Liner, University of Houston

February 26, 2010

Abstract

The continuous wavelet transform utilizing a complex Morlet analyzing wavelet has a close connection to the Fourier transform and is a powerful analysis tool for decomposing broadband wavefield data. A wide range of seismic wavelet applications have been reported over the last three decades, and the free Seismic Unix processing system now contains a code (*succwt)* based on the work reported here.

Introduction

The continuous wavelet transform (CWT) is one method of investigating the time-frequency details of data whose spectral content varies with time (non-stationary time series). Motivation for the CWT can be found in Goupillaud et al. [12], along with a discussion of its relationship to the Fourier and Gabor transforms.

As a brief overview, we note that French geophysicist J. Morlet worked with non-stationary time series in the late 1970's to find an alternative to the short-time Fourier transform (STFT). The STFT was known to have poor localization in both time and frequency, although it was a first step beyond the standard Fourier transform in the analysis of such data. Morlet's original wavelet transform idea was developed in collaboration with theoretical physicist A. Grossmann, whose contributions included an exact inversion formula. A series of fundamental papers flowed from this collaboration [16, 12, 13], and connections were soon recognized between Morlet's wavelet transform and earlier methods, including harmonic analysis, scale-space representations, and conjugated quadrature filters. For further details, the interested reader is referred to Daubechies' [7] account of the early history of the wavelet transform.

Here we describe implementation details of the CWT as applied to wavefield measurements, using reflection seismic data as a specific example. A classic paper in the general field of time-frequency decomposition of reflection seismic data is Chakraborty and Okaya [4]. They discuss the short-time Fourier transform, continuous wavelet transform, discrete wavelet transform, and matched pursuit decomposition, but application to real seismic data is limited to the matched pursuit method.

The CWT implementation described here uses a complex Morlet analyzing wavelet. As a time-domain gaussian-tapered complex exponential, this particular wavelet has a natural and compelling connection to the venerable Fourier transform. An inventory of several

other analyzing wavelets can be found in the excellent summary paper of Torrence and Compo [35].

Fourier Transform

We will use the convention that a time function, $g(t)$, and the Fourier Transform (FT) of that function, $g(\omega)$, are in the time or frequency domain as indicated by the argument list rather than some variation on the function symbol.

The forward FT is defined as usual

$$g(\omega) = \int_{-\infty}^{\infty} g(t)\ e^{i\omega t}\ dt \quad , \tag{1}$$

where scaling constants have been omitted, $i = \sqrt{-1}$, and ω is angular frequency related to linear frequency (f in Hz) by $\omega = 2\pi f$. The function $g(\omega)$ is complex, and can be expressed in polar form $g(\omega) = Ae^{i\theta}$ to reveal the amplitude spectrum, $A(\omega)$, and phase spectrum, $\theta(\omega)$. The inverse FT is given by

$$g(t) = \int_{-\infty}^{\infty} g(\omega)\ e^{-i\omega t}\ d\omega \quad . \tag{2}$$

We define the Dirac delta function heuristically as the unit spike function

$$\delta(t - t_0) = \begin{cases} 1, & t = t_0 \\ 0, & t \neq t_0 \end{cases} \quad . \tag{3}$$

A key feature of $\delta(t)$ is the sifting property it exhibits under the action of integration

$$\int_{-\infty}^{\infty} \delta(t - t_0)\ g(t)\ dt = g(t_0) \quad , \tag{4}$$

It is customary to remark that the FT decomposes a transient time signal (data) into independent harmonic components and, therefore, the function $g(\omega)$ has exact frequency localization and no time localization. In other words, the FT can precisely detect which frequencies reside in the data, but yields no information about the time position of signal features. We can investigate this claim by considering the FT impulse response.

Let $g(t) = \delta(t - t_0)$, take the FT, and apply the sifting property to yield

$$g(\omega) \ = \ \int \delta(t - t_0)\ e^{i\omega t}\ dt \ = \ e^{i\omega t_0} \quad . \tag{5}$$

Recognizing the result is already in polar form, we see the amplitude spectrum, $A = 1$, contains no information about the time location of the spike. The phase, however,

$$\theta = \omega\ t_0 = 2\pi f t_0 \quad , \tag{6}$$

is linear, and the spike location, t_0, is encoded in the phase slope. For this elementary case the spike location can be recovered exactly by

$$t_0 = \frac{1}{2\pi} \frac{d\theta}{df} \quad . \tag{7}$$

More challenging is the case of two spikes

$$g(t) = \delta(t - t_1) + \delta(t - t_2) \tag{8}$$

that transforms to

$$g(\omega) \;=\; e^{i\omega t_1} + e^{i\omega t_2} \tag{9}$$

and which can be written in terms of $\Delta t = t_2 - t_1$ as

$$g(\omega) \;=\; e^{i\omega t_1} \left(1 + e^{i\omega \Delta t}\right) \quad . \tag{10}$$

The accessible spike time information in this function lies in the amplitude rather than the phase spectrum. Specifically, consider the zeros of the amplitude spectrum

$$|g(\omega)| = \left|e^{i\omega t_1}\right| \left|1 + e^{i\omega \Delta t}\right| = 0 \quad . \tag{11}$$

By definition, the first right-side term is never zero, meaning the equality can only hold if

$$\begin{aligned} e^{i\omega \Delta t} &= -1 && (12)\\ i\omega \Delta t &= ln(-1) && (13)\\ i2\pi f_n \Delta t &= i(2n+1)\pi && (14)\\ f_n &= \frac{2n+1}{2\Delta t} \quad ; \quad n = 0, 1, 2, ... && (15) \end{aligned}$$

where f_n is the n^{th} notch frequency. This relationship says that if we can observe the frequency associated with, say, the first spectral notch, f_0, then we can calculate the time separation of the spikes using

$$\Delta t = t_2 - t_1 = \frac{1}{2f_0} \quad . \tag{16}$$

This accomplishment is a muted victory since we do not find the absolute spike times, only the delay between them. Furthermore, even this weak result breaks down if the spikes have different amplitudes (no hard zeros develop in the spectrum), or we move on to the three- or N-spike case. We conclude that although there is some time localization information in the Fourier transform, it quickly becomes an unreasonable exercise to extract it for even simple impulsive time functions.

Something better is needed, and that something is a wavelet transform.

Wavelet Transform

The continuous wavelet transform can be defined in a variety of ways that differ with respect to normalization constants and conjugation. We define the transform as

$$g(a,b) = a^p \int_{-\infty}^{\infty} g(t)\ \psi\left(\frac{t-b}{a}\right)\ dt \quad , \tag{17}$$

where $\psi(t)$ is the analyzing wavelet, b is a time-like translation variable, a is a dimensionless frequency scale variable, and p is a real normalization parameter. As with the FT, we use the argument list to indicate whether $g()$ is in the physical domain, $g(t)$, or the transform domain, $g(a,b)$. This convention is routinely used in geophysics where multidimensional transforms are often encountered [6, 23].

For reconstruction of the original time series, the inverse CWT is in principle given by the double integral

$$g(t) = \int_{-\infty}^{\infty}\int_{-\infty}^{\infty} g(a,b)\ \psi'\left(\frac{t-b}{a}\right)\ da\ db \quad , \tag{18}$$

where the inverse analyzing wavelet ψ' need not be the same as the forward transform wavelet. As discussed by Torrence and Compo [35], if the inverse wavelet is chosen to be a delta function the b integral can be done analytically via the sifting property of the delta function. The inverse is then simplified to the real part of the summation over scales

$$g(t) = Re\left(\int_{-\infty}^{\infty} g(a,t)\ da\right) \quad . \tag{19}$$

Complex Morlet Wavelet

As discussed earlier, the Fourier transform kernel is given by

$$K_{FT} = e^{i2\pi ft} \quad . \tag{20}$$

where $i = \sqrt{-1}$ and f is frequency in Hertz. The kernel in a continuous wavelet transform is simply the analyzing wavelet,

$$K_{CWT} = \psi(t) \quad . \tag{21}$$

For wave-like data a good choice for the analyzing wavele is the complex Morlet wavelet

$$\psi(t) = e^{-(t/c)^2}\ e^{i2\pi f_0 t} \quad , \tag{22}$$

where t is time, f_0 is a frequency parameter, and c is a damping parameter with units of time. This equation describes a time-domain function that is the product of a gaussian and a complex exponential, and whose center frequency is f_0.

The frequency domain representation of the complex Morlet wavelet is

$$\psi(f) = e^{-(cf)^2}\ *\ \delta(f - f_0) \quad , \tag{23}$$

where normalization factors have been omitted, and $*$ denotes convolution. This is, again, a gaussian function, now centered in the frequency domain on f_0.

There are several choices that can be made with respect to wavelet normalization. Our definition, equation 22 along with $p = 0$ in equation 17, normalizes the time-domain peak amplitude.

Comparing the leading terms in equations 22 and 23, we see a duality that expresses the characteristic CWT resolution trade-off. The damping parameter, c, controls the rate at which the time-domain wavelet, and frequency domain spectrum, is driven toward zero. As time localization increases (large c), frequency localization decreases, and vice versa. We have chosen to write the complex Morlet wavelet in this particular form and notation to emphasize the central role of the damping factor. The value of this parameter has a first-order effect on any CWT result. In fact, in the limit as $c \to \infty$ the Morlet wavelet defined here becomes equal to the Fourier kernel.

Figure 1 illustrates the time-frequency resolution properties of the complex Morlet wavelet. In this example, a 60 Hz Morlet wavelet (A) is shown with the real part as a solid line and imaginary part dashed. The damping parameter is $c = 1/120$, resulting in a gaussian-tapered amplitude spectrum (B). Lowering the center frequency to 30 Hz and using $c = 1/60$ gives a wider time-domain wavelet (C) and a narrower frequency spectrum (D). It should be noted, that these results are not dependent on the absolute size of the frequencies being considered, similar plots could be constructed for 60 and 30 MHz.

Note the choice of damping parameter in Figure 1 as the inverse of twice the center frequency of the wavelet. Using this value will preserve a wavelet time span equal two times its period.

When used to compute the CWT, the argument of the analyzing wavelet (equation 22) is translated and scaled, $\psi\left(\frac{t-b}{a}\right)$. The effect of scaling is two-fold. In the real exponential, the scale value multiplies the damping parameter, effectively broadening the time-domain extent of the wavelet. In the complex exponential, the scale divides the frequency, lowering it precisely enough to maintain the number of time-domain oscillations.

Scales and Frequencies

The continuous wavelet transform represented by equation 17 is related to convolution as evidenced by the appearance of $(t - b)$ in the integral. Thus, the CWT can be written as

$$g(a, t) = g(t) * \psi(t/a) \quad , \tag{24}$$

showing the CWT can be implemented as a series of complex-valued time domain convolutions. Each convolution involves the input data and a version of the analyzing wavelet modified by the scaling variable. Strictly speaking, the CWT is an inner product, or the zero lag of a complex-valued correlation, that can be expressed as a convolution under certain symmetry conditions. The CWT as a cross-correlation is understandable since we are matching similarities between the signal and the analyzing wavelet.

From a computational point of view, complex time-domain convolutions are highly inefficient. The mathematical form of equation 24 suggests implementation in the Fourier

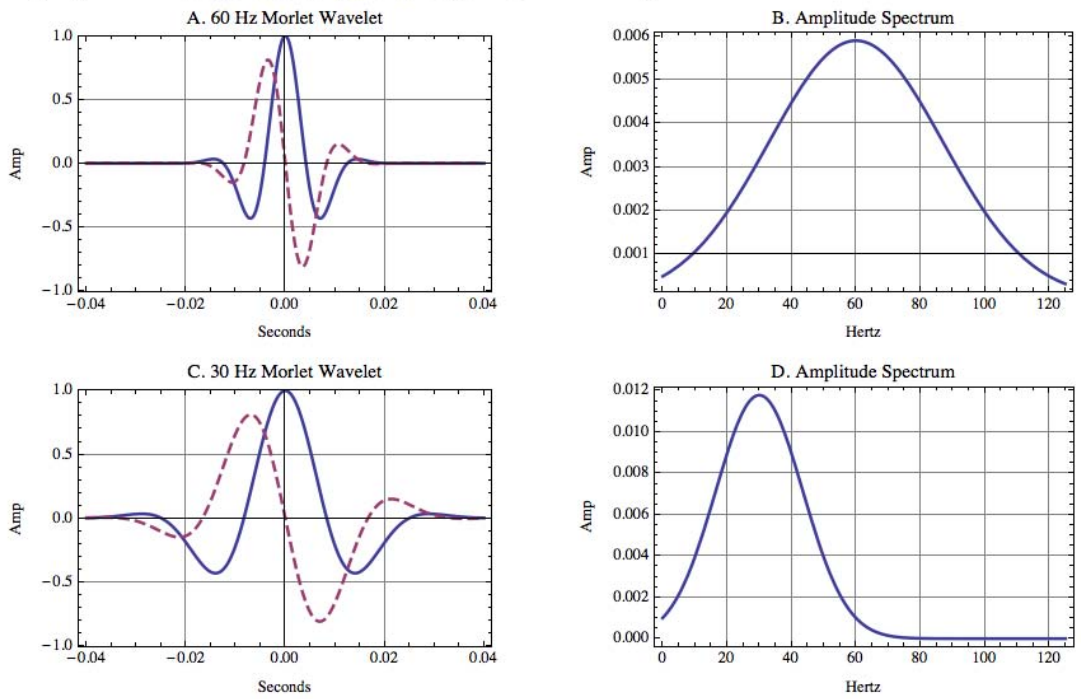

Figure 1: Complex Morlet wavelet in the time and frequency domain. (A) 60 Hz Morlet wavelet showing real (solid) and imaginary (dash) parts. The damping parameter is $c = 1/120$. (B) Fourier amplitude spectrum of the 60 Hz Morlet wavelet showing characteristic gaussian shape. (C) A 30 Hz Morlet wavelet ($c = 1/60$) has longer time duration, but the same number of oscillations. (D) The amplitude spectrum of the 30 Hz wavelet is narrower because the time-domain function is wider.

domain where the convolution will become multiplication. Recalling the Fourier transform scaling property for a general time function $g(t)$

$$FT\{g(t/a)\} = a\ g(af) \quad , \tag{25}$$

we can write equation 24 in the Fourier domain as the compact and efficient result

$$g(a,t) = FT^{-1}\{a\ g(f)\ \psi(af)\} \quad . \tag{26}$$

A fundamental contribution of Morlet's early work [12] was recognition that the natural sampling of this scale variable is dyadic (i.e., logarithmic, base 2). If the wavelet is dilated by a factor of 2, this means the frequency content has been shifted by one octave. The analogy with music and singing clear, and is perpetuated by defining the scale range in terms of octaves and voices. The number of octaves determines the span of frequencies being analyzed, while the number of voices per octave determines the number of samples (scales) across this span.

Specifically, let the number of octaves in a CWT be N_o and the number of voices per

octave be N_v. The octave and voice indices progress as

$$i_o = 0, 1, 2, ..., N_o - 1 \quad (27)$$
$$i_v = 0, 1, 2, ..., N_v - 1 \quad . \quad (28)$$

The scale value for a given octave i_o and voice i_v is given by

$$a = 2^{(i_o + i_v/N_v)} \quad , \quad (29)$$

and it follows that the smallest scale value is 1 and the largest is

$$a = 2^{(N_o - 1/N_v)} \quad . \quad (30)$$

The scales are referenced to an index that progresses as

$$i_a = 1, 2, ..., N_o \; N_v \quad . \quad (31)$$

that can be calculated with the scales themselves by the double loop

```
ia = 1
for io = 0, No - 1 {
     for iv = 0, Nv - 1 {
          a(ia) = 2^(io+iv/Nv)
          ia = ia + 1
     }
}
```

that can be precomputed before any convolutions are performed.

The appropriate range of octaves and scales depends on the spectral content of the data, and the highest requested frequency in the CWT. In this paper we will always take the highest CWT frequency to be the Nyquist frequency. This is a safe choice, but there is some minor inefficiency because data is usually sampled in such a way that nyquist is well above the highest signal frequency.

We now have the components necessary to relate scales and frequencies. Consider a CWT consisting of 5 octaves and 10 voices per octave. Figure 2A shows a plot of scale index versus scale value for this case. The scale values range from 1 ($i_a = 1$) to 29.86 ($i_a = 50$). To associate a frequency with each scale, we must specify the maximum frequency in the CWT transform, which is also the initial frequency of the analyzing wavelet. Lower frequencies are generated when this initial frequency is divided by successive scale factors. Using a typical seismic example of $dt = .004$ seconds, the Nyquist frequency is 125 Hz and the scale values map into frequencies as shown in Figure 2B. We will retain this scale-frequency relationship in the examples that follow. It must always be remembered that a CWT scale does not correspond to a single Fourier frequency, a gaussian spectrum peaked at the Morlet central frequency.

By choosing 5 octaves descending from a Nyquist frequency of 125 Hz, the lowest frequency in the CWT is $125/29.86 = 4.2$ Hz. Typical acquisition procedures for petroleum

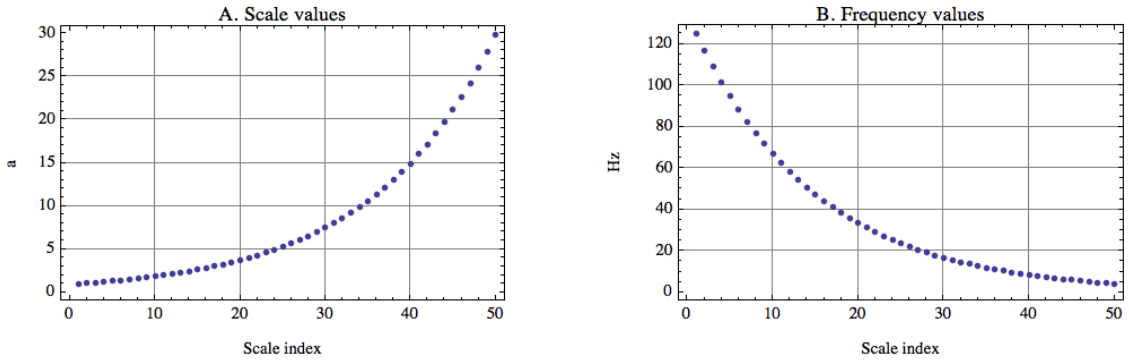

Figure 2: Relationship between scale values and frequencies. (A) Plot of scale index versus scale value for a 5 octave, 10 voice continuous wavelet transform. (B) By assuming the highest frequency in the transform is Nyquist (125 Hz in this case), each scale can be associated with a particular frequency.

seismic data does not preserve frequencies below 5 Hz, so we conclude that a 5-octave transform should adequately span the spectral content of such data.

One last implementation detail is specification of the damping parameter, c, discussed earlier in relation to the Morlet wavelet definition (equation 22). If dt is the time sample rate, and the highest CWT frequency is Nyquist, and we want one full expression of the wavelet (no more) at every scale, then the appropriate value is $c = dt$. This gives fine time-localization of the CWT, at the expense of poor frequency resolution. In applications requiring better frequency localization a larger value of c should be used. A version of the CWT described here is available as *succwt* (source code succwt.c) in the Seismic Unix processing system [5].

Figure 3 illustrates the response of a 5 octave, 10 voice CWT to impulse data. The data (A) consists of zero values except for a unit amplitude spike at one point. The real part of the $c = 0.004$ CWT impulse response (B) is a time-localized feature that becomes progressively lower-frequency at larger scales. This is consistent with the scale-frequency mapping in Figure 2. The maximum amplitude on each scale trace is shown, confirming our choice to normalize the transform on time-domain peak amplitude ($p = 0$ in equation 17). The $c = 0.008$ CWT impulse response (C) shows more oscillations in the analyzing wavelet leading to more frequency localization.

A sense of the broad range of seismic topics amenable to wavelet transform analysis can be gained from Table 1. This list shows published applications along with the author name(s) and year. Only the first occurrence of any particular application is reported. It is derived from the citation search index maintained by the Society of Exploration Geophysicists (SEG). This index [33] includes publications of the SEG, Canadian SEG, Australian SEG, and European Association of Geoscientists and Engineers.

Any such compilation is limited. Significant workers in the field (such as J. Morlet, A. Chakraborty, and F. Herrmann, to mention a few) may not be represented if they worked in

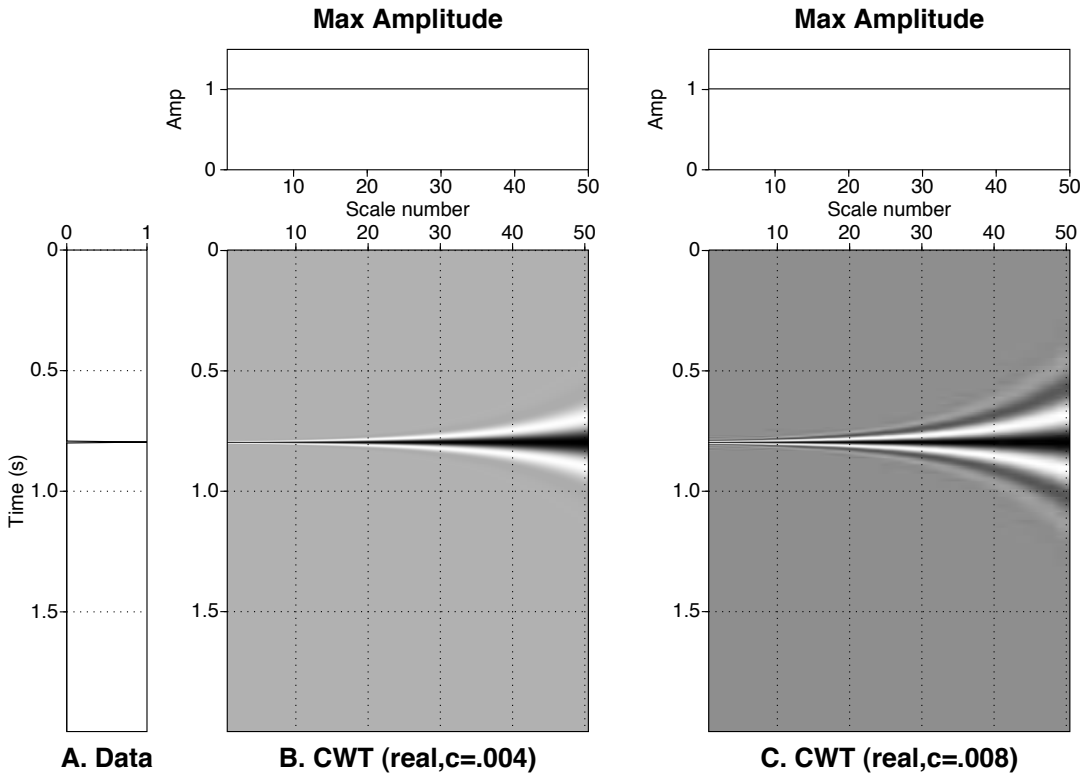

Figure 3: Continuous wavelet transform (CWT) impulse response. (A) Input data consisting zero values and one unit-amplitude spike. There are 500 time samples and the time sample rate is $dt = .004$ seconds. (B) Real part of the CWT of the data using $c = 0.004$. This is a 5 octave, 10 voice CWT with maximum frequency of 125 Hz (Nyquist). The scale axis is associated with frequency through Figure 2. (C) Impulse response using $c = .008$.

fundamental, rather than applied, areas of the subject. Also, keyword searches are fragile, a search on 'wavelet transform' may not catch a title containing 'wavelet-packet transform'. That being said, the table probably does a fair job of representing range and progress of wavelet transform applications to reflection seismology data.

Examples

Figure 4 illustrates the kind of result CWT produces from reflection seismic data. The data (A) is a marine 2D seismic section from offshore Thailand consisting of 200 migrated traces. Each trace is 2 seconds long with time sample rate of $dt = .004$ s. The sea floor is clearly visible, along with subsurface geologic features including faults and stratigraphic terminations. A 5 octave, 10 voice CWT ($c = .004$) is computed from the center trace

and the amplitude spectrum is displayed (B). The scale axis corresponds to frequencies in accordance with Figure 2.

As discussed earlier, we have chosen Nyquist to be the highest frequency in the transform. Note the decay in amplitude beyond scale 45, indicating that our choice of 5 octaves does, indeed, span the low frequency content of this data. One immediate observation is the decay of bandwidth experienced by seismic waves that have travelled farther through the earth. The sea floor reflection has significant energy from scales 45-8 (8-75 Hz), while the deepest reflectors are limited to scales 45-15 (8-50 Hz) due to loss of high frequencies by scattering and attenuation processes [23]. It follows that the CWT is a natural tool for estimating subsurface attenuation.

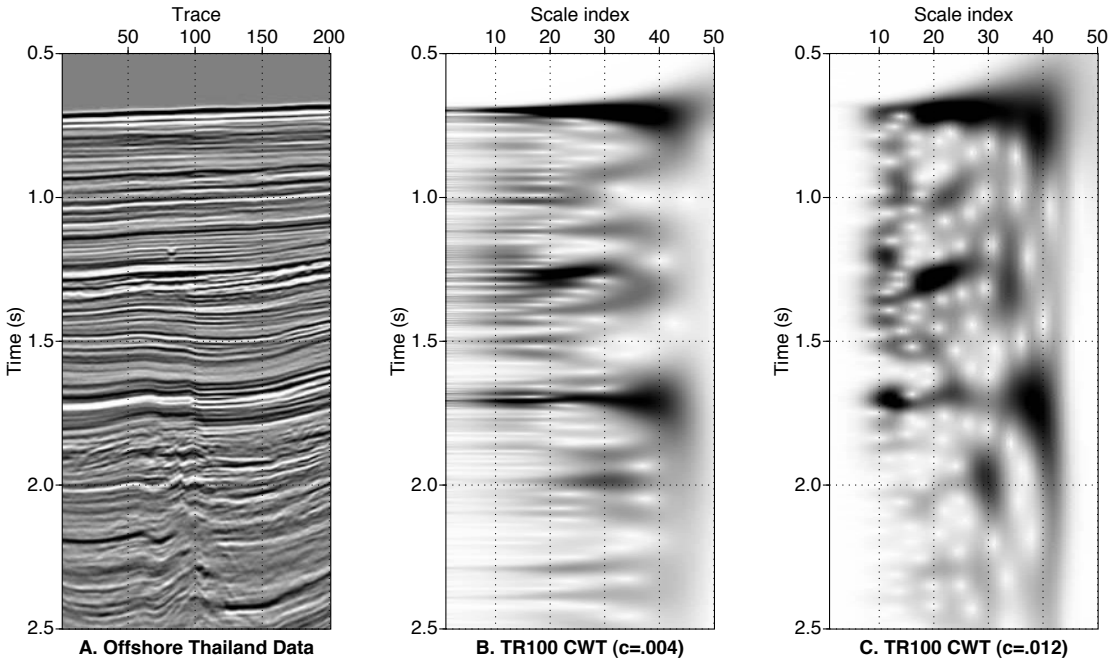

Figure 4: CWT of seismic data. (A) Migrated 2D seismic section. (B) CWT amplitude spectrum of center trace ($c = 0.004$) (C) CWT amplitude spectrum of center trace ($c = 0.004$)

Although we can see the loss of bandwidth, the appearance of this CWT result is strongly influenced by the damping parameter. With a value of $c = 0.004$, the CWT has maximum time-localization but very poor frequency resolution. Computing the CWT with $c = .012$ gives the result in Figure 4C. The bandwidth changes are more easily observed, along with spectral notches associated with thin bed interference effects. These develop as more oscillations are allowed in the analyzing wavelet.

By computing a CWT like the one shown in Figure 4 for every trace in a 3D migrated seismic volume, we would generate a 4D volume of data whose coordinates are time, x-bin, y-bin, and scale. From this a series of seismic 3D volumes could be extracted, each corre-

sponding to a unique center frequency. This is the concept of the spectral decomposition seismic attribute [15], although it should be mentioned there are methods available that isolate individual frequencies better than the CWT. In petroleum seismology, attributes are data types computed from primary amplitude data to visually enhance or isolate features of interest, or calibrated to borehole measurements for reservoir property prediction.

Figure 5 shows an example of CWT spectral decomposition. The broadband data (A) is a small subset of the offshore Thailand data. This section begins just below the sea floor. From Fourier analysis, we find the frequency content is 8-72 Hz which gives a dominant frequency of 40 Hz. Scale 15 of the CWT spectrum in Figure 4 represents a narrow band 50 Hz version of one input trace. Repeating this for all input traces, we can display a narrow band expression of the seismic line, as shown in Figure 5B. Note that two intervals between 1.5-2.0 seconds show anomalous behavior in the 50 Hz result. The value of spectral decomposition is that, when calibrated to well control, such anomalies may be associated with hydrocarbon reservoirs.

One of the great strengths of the CWT is the vast body of theoretical work associated with it. It is more than just another time-frequency spectrum. Our second application example, the Spice attribute [18], draws on this theoretical work, specifically regularity analysis and the Hölder exponent.

To a skilled seismic interpreter the data in Figure 5A tells a story of faulting, unconformities, and stratigraphy. In the mind of such an interpreter, a subsurface model would evolve through long and detailed analysis of the seismic image. The Spice attribute (Figure 5C) represents an automated step toward that subsurface model. Where the seismic image is a composite of many interfering thin bed reflection events and amplitude oscillations, the Spice result is a stratified subsurface model consistent with the observed data. As the global search for petroleum demands better ways to extract information from seismic data, Spice, and wavelet attributes yet undiscovered, are sure to play a role.

Conclusions

The continuous wavelet transform (CWT) utilizing a complex Morlet analyzing wavelet has a close connection to the Fourier transform and is a powerful analysis tool for decomposing broadband wavefield data. Care must be taken in choosing the range of octaves in the transform, and particular attention must be paid to the time-domain gaussian damping parameter.

Applied to reflection seismic data, the CWT can form the basis of spectral decomposition or more exotic attributes such as Spice. A wide range of seismic wavelet applications have been reported over the last three decades, and there is a trend related to development of advanced interpretation tools. We anticipate quickening of this rate of innovation as wavelet methods, move into general use. To aid this development, the free Seismic Unix processing system now contains a code succwt based on the work reported here.

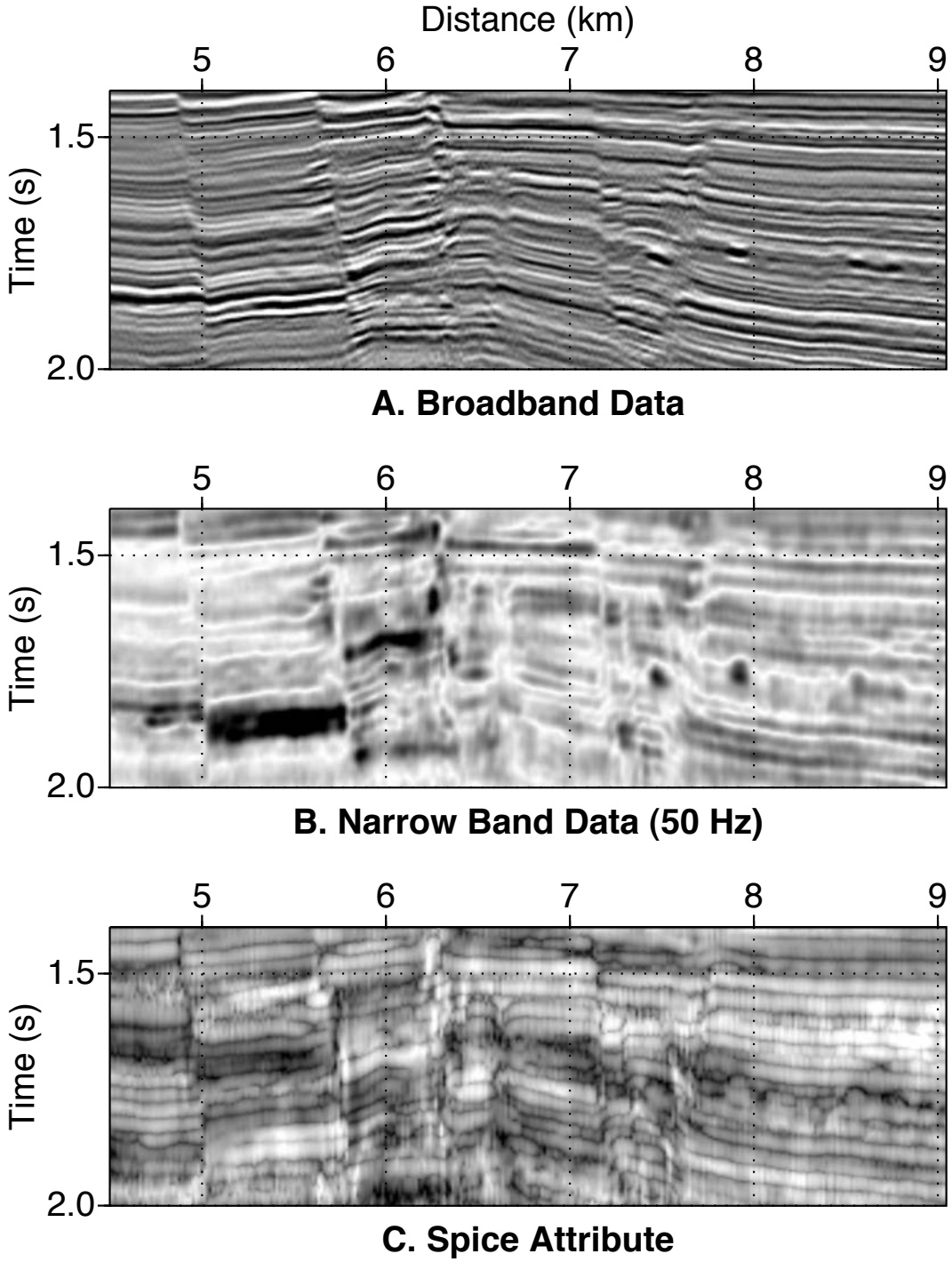

Figure 5: Spectral decomposition and Spice. (A) Migrated 2D seismic section. (B) Narrow-band data with center frequency of 50 Hz showing anamolous zones (dark). (C) Spice attribute computed from the input data visualizes subsurface layering.

Acknowledgements

The author wishes to acknowledge early discussions with Chun-Feng Li., and thank James Childress (U. Tulsa) and Robert Clapp (Stanford) for programming help.

Application	**Author**	**Ref**	**Year**
Downward continuation	LeBras et al.	[17]	1992
Shear wave discrimination	Niitsuma et al.	[27]	1993
Seismic data processing	Miao and Moon	[26]	1994
Wavefield extrapolation	Dessing and Wapenaar	[10]	1994
Wave equation inversion	Yang and Qian	[40]	1994
Data compression	Reiter and Heller	[30]	1994
Trace interpolation	Wang and Y. Li	[37]	1994
Phase quality control	Asfirane et al.	[1]	1995
Migration	Dessing and Wapenaar	[11]	1995
Tomography	X. Li and Ulrych	[21]	1995
Sonic velocity characterization	X. Li and Haury	[19]	1995
Compressed migration	Wang and Pann	[38]	1996
Hilbert attribute analysis	X. Li and Ulrych	[22]	1996
Singularity analysis	Cao	[2]	1996
Signal-to-noise and resolution	K. Li et al.	[20]	1996
Deconvolution	Marenco and Madisetti	[25]	1996
Edge detection	Dessing et al.	[9]	1996
Velocity filtering	Deighan and Watts	[8]	1997
Reflection tomography	Carrion	[3]	1997
Borehole data upscaling	Verhelst and Berkout	[36]	1997
Spectral decomposition	Gridley and Partyka	[15]	1997
Amplitude versus offset	Wapenaar	[38]	1997
Reflector characterization	Goudswaard and Wapenaar	[14]	1998
3D seismic sequence analysis	Yin et al.	[41]	1998
Thin bed analysis	Zhu and Q. Li	[42]	1999
Complex media characterization	Pivot et al.	[29]	1999
Direct hydrocarbon detection	Sun et al.	[34]	2002
Reservoir characterization	Osorio et al.	[28]	2003
Time-frequency attribute	Sinha et al.	[31]	2003
Spice attribute	C.-F. Li and Liner	[32]	2004
Group velocity imaging	Liner, Bell, and Verm	[24]	2009

Table 1: Some published applications of the wavelet transform to petroleum seismic data.

Bibliography

References

[1] Asfirane, F., Rodriguez, J. -M. and Julien, P., 1995, Phase quality data control using the wavelet transform, 57th Mtg.: Eur. Assn. of Expl. Geophys., Session:P061.

[2] Cao, Y., 1996, Singularity feature analysis of seismic traces, 66th Ann. Internat. Mtg: Soc. of Expl. Geophys., 1619-1622.

[3] Carrion, P., 1997, Reflection tomography in wavelet transform domain, 59th Mtg.: Eur. Assn. Geosci. Eng., Session:E035.E035.

[4] Chakraborty, A. and Okaya, D., 1995, Frequency-time decomposition of seismic data using wavelet-based methods: Geophysics, Soc. of Expl. Geophys., 60, 1906-1916.

[5] Cohen, J. K. and Stockwell, Jr. J. W., (2010), CWP/SU: Seismic Un*x Release No. 42: an open source software package for seismic research and processing, Center for Wave Phenomena, Colorado School of Mines.

[6] Claerbout, J. F., 1985, Imagining the Earth's Interior, Blackwell Scientific Publications, London.

[7] Daubechies, I., 1996, Where do wavelets come from?—A personal point of view, Proceedings of the IEEE Special Issue on Wavelets 84 (4), 510-513.

[8] Deighan, A. J. and Watts, D. R., 1997, Ground-roll suppression using the wavelet transform: Geophysics, Soc. of Expl. Geophys., 62, 1896-1903.

[9] Dessing, F. J., Hoekstra, E. V., Herrmann, F. J. and Wapenaar, C. P. A., 1996, Multiscale edge detection by means of multiscale migration, 66th Ann. Internat. Mtg: Soc. of Expl. Geophys., 459-462.

[10] Dessing, F. J. and Wapenaar, C. P. A., 1994, Wavefield extrapolation using the wavelet transform, 64th Ann. Internat. Mtg: Soc. of Expl. Geophys., 1355-1358.

[11] Dessing, F. J. and Wapenaar, C. P. A., 1995, Efficient migration with one-way operators in the wavelet transform domain, 65th Ann. Internat. Mtg: Soc. of Expl. Geophys., 1240-1243.

[12] Goupillaud, P. L., Grossmann, A. and Morlet, J., 1984, A simplified view of the cycle-octave and voice representations of seismic signals, 54th Ann. Internat. Mtg: Soc. of Expl. Geophys., Session:S1.7.

[13] Goupillaud, P., Grossman, A., and Morlet. J., 1984, Cycle-Octave and Related Transforms in Seismic Signal Analysis. Geoexploration, 23, 85-102.

[14] Goudswaard, J. C. M. and Wapenaar, K., 1998, Characterization of reflectors by multi-scale amplitude and phase analysis of seismic data, 68th Ann. Internat. Mtg: Soc. of Expl. Geophys., 1688-1691.

[15] Gridley, J. and Partyka, G., 1997, Processing and interpretational aspects of spectral decomposition, 67th Ann. Internat. Mtg: Soc. of Expl. Geophys., 1055-1058.

[16] Grossmann, A., and Morlet, J., 1984, Decomposition of Hardy functions into square integrable wavelets of constant shape. SIAM J. Math. Anal., 15, 723-736, 1984

[17] LeBras, R., Mellman, G. and Peters, M., 1992, A wavelet transform method for downward continuation, 62nd Ann. Internat. Mtg: Soc. of Expl. Geophys., 889-892.

[18] Li, C.-F., and Liner, C., 2008, Wavelet-based detection of singularities in acoustic impedances from surface seismic reflection data, Geophysics,73,V1

[19] Li, X. -P. and Haury, J. C., 1995, Characterization of heterogeneities from sonic velocity measurements using the wavelet transform, 65th Ann. Internat. Mtg: Soc. of Expl. Geophys., 488-491.

[20] Li, K., Liu, Y. and Li, Y., 1996, Improving both seismic section signal-noise ratio and resolution by the properties of wavelet transform zero-crossings and polynomial fitting, 66th Ann. Internat. Mtg: Soc. of Expl. Geophys., 1446-1449.

[21] Li, X. -G. and Ulrych, T. J., 1995, Tomography via wavelet transform constraints, 65th Ann. Internat. Mtg: Soc. of Expl. Geophys., 1070-1073.

[22] Li, X. -G. and Ulrych, T. J., 1996, Multi-scale attribute analysis and trace decomposition, 66th Ann. Internat. Mtg: Soc. of Expl. Geophys., 1634-1637.

[23] Liner C., 2004, Elements of 3D Seismology, Second Edition, Pennwell Publishing Co., Tulsa, OK.

[24] Liner, C., Bell, L., and Verm, R., 2009, Direct imaging of group velocity dispersion curves in shallow water SEG, Expanded Abstracts,28,3317

[25] Marenco, A. L. and Madisetti, V. K., 1996, Deconvolution of seismic traces using homomorphic analysis and matching pursuit, 66th Ann. Internat. Mtg: Soc. of Expl. Geophys., 1188-1191.

[26] Miao, X. G. and Moon, W. M., 1994, Application of the wavelet transform in seismic data processing, 64th Ann. Internat. Mtg: Soc. of Expl. Geophys., 1461-1464.

[27] Niitsuma, H., Tsuyuki, K. and Asanuma, H., 1993, Discrimination of split shear waves by wavelet transform: J. Can. Soc. Expl. Geophys., 29, no. 01, 106-113.

[28] Osrio, P.L.M., Matos, M. C. and Johann, P. R. S., 2003, Using Wavelet Transform and Self Organizing Maps for Seismic Reservoir Characterization of a Deep-Water Field, Campos Basin, Brazil, 65th Mtg.: Eur. Assn. Geosci. Eng., B29.

[29] Pivot, F., Guilbot, J. and Bernet-Rollande, O., 1999, Continuous wavelet transform as a tool for complex media characterisation, 61st Mtg.: Eur. Assn. Geosci. Eng., Session:6029.

[30] Reiter, E. C. and Heller, P. N., 1994, Wavelet transform-based compression of NMO-corrected CDP gathers, 64th Ann. Internat. Mtg: Soc. of Expl. Geophys., 731-734.

[31] Sinha, S., Routh, P., Anno, P. and Castagna, J., 2003, Time-frequency attribute of seismic data using continuous wavelet transform, 73rd Ann. Internat. Mtg.: Soc. of Expl. Geophys., 1481-1484.

[32] Smythe, J., Gersztenkorn, A., Radovich, B., Li C.-F., and Liner C., 2004, Gulf of Mexico shelf framework interpretation using a bed-form attribute from spectral imaging The Leading Edge,23,921

[33] Society of Exploration Geophysicists, 2004, `http://seg.org/searches/dci.shtml`

[34] Sun, S., Siegfried, R. and Castagna, J., 2002, Examples of wavelet transform time-frequency analysis in direct hydrocarbon detection, 72nd Ann. Internat. Mtg: Soc. of Expl. Geophys., 457-460.

[35] Torrence, C. and Compo, G., 1998. A practical guide to wavelet analysis. Bulletin of the American Meteorological Society 79 (1), 61-78.

[36] Verhelst, F. and Berkhout, A. J., 1997, Comparison of seismic and borehole data at the same scale, 67th Ann. Internat. Mtg: Soc. of Expl. Geophys., 830-833.

[37] Wang, Z. and Li, Y., 1994, Trace interpolation using wavelet transform, 64th Ann. Internat. Mtg: Soc. of Expl. Geophys., 729.

[38] Wang, B. and Pann, K., 1996, Kirchhoff migration of seismic data compressed by matching pursuit decomposition, 66th Ann. Internat. Mtg: Soc. of Expl. Geophys., 1642-1645.

[39] Wapenaar, C. P. A., 1997, Multi-scale AVA analysis, 67th Ann. Internat. Mtg: Soc. of Expl. Geophys., 218-221.

[40] Yang, F. and Qian, S., 1994, 3-D viscoelastic wave equation inversion: Application of wavelet transform , 64th Ann. Internat. Mtg: Soc. of Expl. Geophys., 1046-1048.

[41] Yin, X., Wu, G. and Qu, S., 1998, Application of wavelet transform in 3-D seismc sequence analysis, 68th Ann. Internat. Mtg: Soc. of Expl. Geophys., 649-652.

[42] Zhu, G. and Li, Q., 1999, The wavelet transform and thin bed analysis, 61st Mtg.: Eur. Assn. Geosci. Eng., Session:P002.